Advanced Robotics

ISSN: 0169-1864 (Print) 1568-5535 (Online) Journal homepage: http://www.tandfonline.com/loi/tadr20

Pneumatic impedance control of a 3-d.o.f. physiotherapy robot

R. Richardson , A. Jackson , P. Culmer , B. Bhakta & M. C. Levesley

To cite this article: R. Richardson , A. Jackson , P. Culmer , B. Bhakta & M. C. Levesley (2006) Pneumatic impedance control of a 3-d.o.f. physiotherapy robot, Advanced Robotics, 20:12, 1321-1339, DOI: 10.1163/156855306778960590

To link to this article: https://doi.org/10.1163/156855306778960590

Published online: 02 Apr 2012.

Advanced Robotics, Vol. 20, No. 12, pp. 1321–1339 (2006)

Also available online - www.brill.nl/ar

Full paper

Pneumatic impedance control of a 3-d.o.f. physiotherapy robot

R. RICHARDSON [1,*], A. JACKSON [2], P. CULMER [2], B. BHAKTA [3] and M. C. LEVESLEY [2]

[1] *School of Computer Science, University of Manchester, Manchester M13 9PL, UK*
[2] *School of Mechanical Engineering and* [3] *Rheumatology and Rehabilitation Research Unit, School of Medicine, University of Leeds, Leeds LS2 9JT, UK*

Received 20 May 2005; accepted 11 August 2005

Abstract—Stroke is a common condition resulting in 30 000 people per annum left with significant disability. In patients with severe arm paresis after stroke, functional recovery in the affected arm is poor. Inadequate intensity of treatment is cited as one factor accounting for the lack arm recovery found in some studies. Given that physical therapy resource is limited, strategies to enhance the physiotherapists' efforts are needed. One approach is to use robotic techniques to augment movement therapy. A 3-d.o.f. pneumatic robot has been developed to apply physiotherapy to the upper limb. The robot has been designed with a workspace encompassing the reach-retrieve range of the average male. Slight non-linearities in the response of the pneumatic system are observed and explained. Building upon previous work that used an error-prone custom force sensor, a commercial 6-d.o.f. force sensor is used to apply impedance control in 3 d.o.f. on the robot.

Keywords: Impedance control; pneumatic cylinders; robotic physiotherapy.

NOMENCLATURE

x, y, z	displacement (m)
F_x, F_y, F_z	force respective to x, y and z (N)
V_x, V_y, V_z	voltages from force sensor (V)
C_{Q}	matrix of calibration coefficients
θ_3	angular displacement (rad)
K_{op}	open-loop force control gain
M	inertia
C	damping (N/m^2)

*To whom correspondence should be addressed. E-mail: R.C.Richardson@cs.man.ac.uk.

K	stiffness (N/m)
x_{d}	position demand (m)
x_{p}, y_{p}, z_{p}	global desired positions (m)
x_{i}, y_{i}, z_{i}	impedance trajectory (m)
θ_1, θ_2, θ_3	joint space demands (rad)
τ_{ex1}, τ_{ex2}, τ_{ex3}	torque on links due to external force

1. INTRODUCTION

Stroke is a common condition (annual incidence 2 per 1000) and a major cause of morbidity with 35% of patients left disabled [1]. Among those admitted with arm paresis, recovery in the arm is generally poor and has a major impact on self-care. A major component of arm rehabilitation after stroke is physical therapy. There is some evidence for a beneficial effect of physical therapy on recovery of the arm with a positive dose–response relationship [2, 3]. Even in rehabilitation services that purport to deliver an intensive program of physical therapy to patients with stroke, the amount of intervention may be inadequate because patients spend a large proportion of time not engaged in 'rehabilitation' activities [4]. Given that physical therapy resource is severely limited, strategies to enhance the physiotherapist's efforts are needed. One approach is the use of robotic techniques to augment physical therapy.

Cozens [5] was the first to demonstrate responsive robotic assistance during an active patient arm exercise. Recently, several research groups have been investigating development prototype robotic devices that have the potential to apply precise, quantifiable and repeatable movement therapy to stroke patients; however, current prototypes tend to be complex and expensive [6–8]. The high power-to-weight ratio, low cost and direct-drive capabilities of pneumatic actuators mean that the potential exists to make such devices simpler and more affordable.

For a robot to administer physiotherapy it is connected directly to a human, whist considering both the force applied and its position. It is not possible to control force and position simultaneously; however, several strategies for moderating force and position have been developed. The three main strategies are: hybrid force and position control, parallel force and position control, and impedance control. The hybrid force and position control strategy [9] controls force and position in orthogonal directions, enabling separate force and position controllers to be implemented on multi-degree-of-freedom (d.o.f.) systems. The parallel force and position control strategy [10] also controls the force and position in orthogonal directions, but does not require predetermined knowledge of the environmental constraints. Both these controllers would behave solely as a force-controller in this physiotherapy context due to contact always being maintained in all d.o.f. between the robot and human. The impedance control strategy [11] does not control the position or force, but rather the dynamic relationship between the two. This enables a compromise between the two conflicting demands. The control aim is to change the manipulator end-point behavior so its force and position relationship is given by a simple mass, spring and damping arrangement. It has been shown that this strategy is appropriate for a robotic physiotherapy device [6].

In any robotic device the actuators are normally the most significant component in terms of the device cost and effectiveness. Traditionally, pneumatic actuators were considered to be only useful for end stop positioning (fully extended or contracted). However, recent developments in pneumatic systems enable them to be considered for applications where previously only hydraulic systems or electric motors were suitable [12–15]. Few researchers have investigated force and position control strategies on pneumatic systems, mainly due to control difficulties caused by air compressibility. Impedance control applications, where low stiffness is required, can be difficult to implement on robots actuated by electric motors due to backlash and friction. In this instance, air compressibility is actually beneficial since it can enable smoother, more supple motion. Gorce and Guihard [16] have designed and simulated a multi-d.o.f. pneumatic impedance control strategy, where a pneumatic force model was used to control the force output of individual pneumatic cylinders. However, the difficulty of experimentally implementing accurate force control of pneumatic cylinders during motion should not be underestimated, with factors such as stiction and air compressibility combining to degrade the system performance. Indeed, Heinrichs *et al.* [17] found that an impedance controller based around position control was more appropriate during implementation on a hydraulic manipulator. Preliminary work on a single-d.o.f. position-based impedance controller has demonstrated good results [18], this work has been extended using a custom 3-d.o.f. force sensor to investigate robotic physiotherapy [21]. The customized force sensor misinterpreted torque input as force therefore greatly restricting its usefulness.

This paper builds upon previous work [21] by explaining in detail the pneumatic system the robot implements and applies a commercial 6-d.o.f. force sensor. The commercial force sensor enabled accurate measurement of external forces in the presence of torques. The work described in Ref. [21] found that making the assumption torque could be neglected by a ball joint connection between the human arm and robot was not valid. The results presented in this paper demonstrate greater accuracy, a larger range of allowable impedance parameters and, most importantly, the results are not affected by applied torque.

The remainder of the paper is structured as follows. Section 2 details the pneumatic components consisting of a 3-d.o.f. pneumatically actuated robot and analyzes the pneumatic system. Section 3 demonstrates the performance of an impedance controller in 3-d.o.f. on the robot with input force measured by a 6-d.o.f. force and torque sensor. Section 4 discusses the work and draws conclusions from it.

2. EXPERIMENTAL APPARATUS

The experimental equipment consists of three parts: a 3-d.o.f. prototype physiotherapy robot, the pneumatic actuation system and the 3-d.o.f. force sensor. An overview of all the system components is given in Table 1.

2.1. The prototype physiotherapy robot

Conclusions drawn from design and development of a single-d.o.f. physiotherapy robot indicated that robotic physiotherapy has many potential benefits; however, applications for single-d.o.f. movement are limited [19].

A 3-d.o.f. pneumatically actuated robot has therefore been designed and constructed (Fig. 1) to take into account the optimum reach range of the average hu-

Table 1.
Equipment specifications

Component	Properties
3 × Low-friction pneumatic cylinder (Airpot Airpel—Air bearing design)	bore 0.627 in. stroke: 6 in.
6 × Electro-pneumatic pressure control valves (SMC E-P Hyreg VY1100)	pressure range: 0–8.8 bar voltage range: 1–5 V
ATI industrial automation SI-20-1 (6-d.o.f. force/torque sensor)	F_x, F_y, = ±20 N, F_z = ±60 N, T_x, T_y, T_z = ±1 N/m
2 × National Instruments DAC cards	1 × 16 input/2 output 1 × 6 output

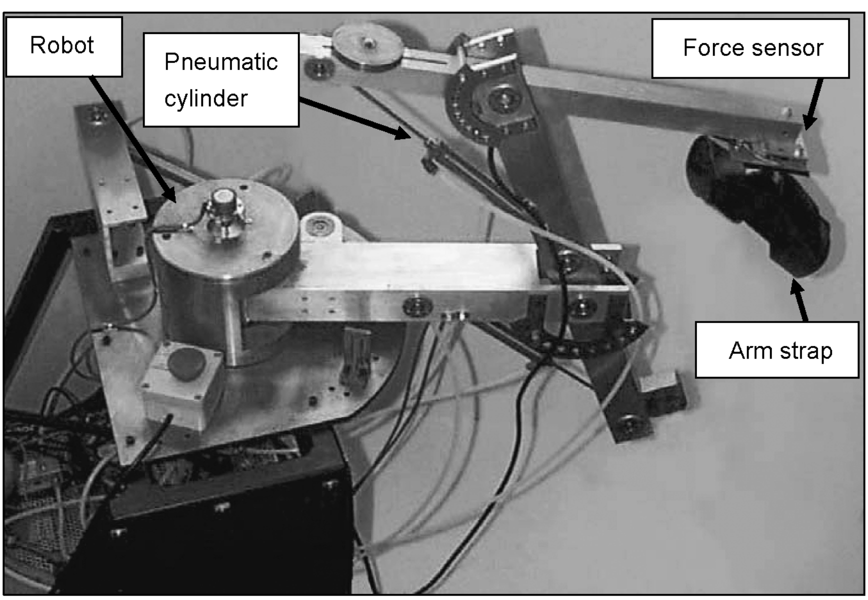

Figure 1. The 3-d.o.f. pneumatic physiotherapy robot.

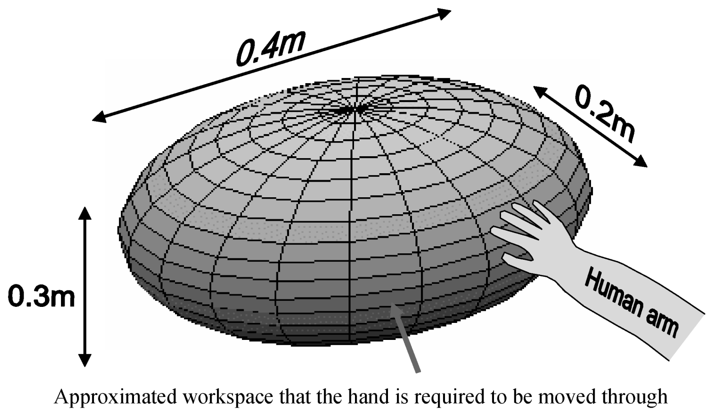

Figure 2. Ergonomic operational range.

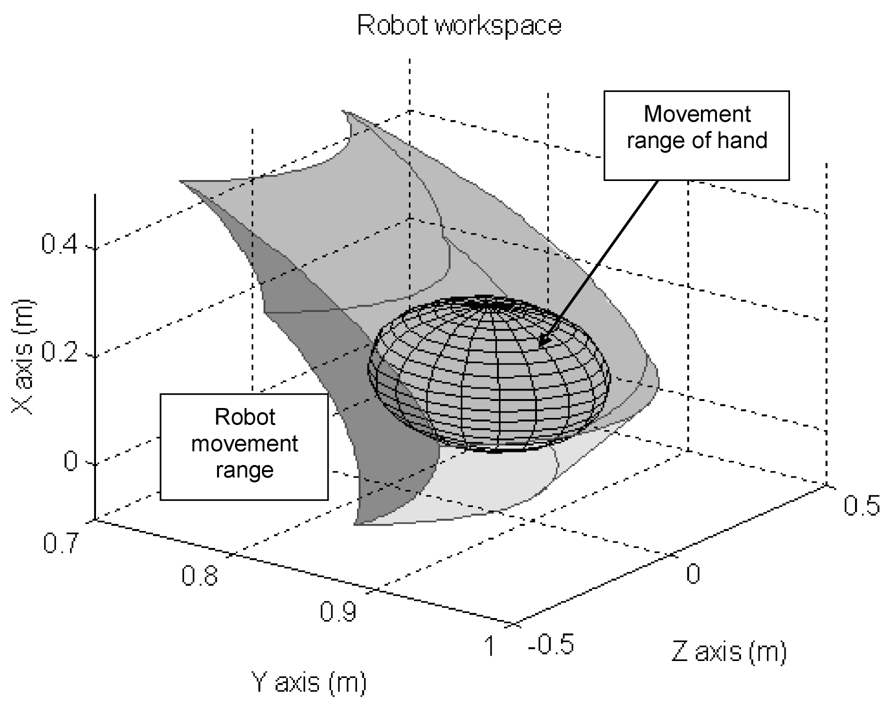

Figure 3. Robot workspace.

man. This can be approximated as the volume shown in Fig. 2 [20]. The robot has been designed so that its operational workspace encompasses this 'optimum range' of hand motions (Fig. 3). Previous work implemented a custom-built force sensor to measure contact forces. Limitations in this force sensor resulted in torque being misread as force [21]. In this work, a commercial force sensor has been implemented on the robot with greatly improved robustness and accuracy.

2.2. Pneumatic system

A pneumatic consisting of a low-friction pneumatic cylinder and two electro-pneumatic valves actuation system provides the actuation force for the robot. The low-friction cylinder minimizes stiction effects enabling accurate control [14] and each valve supplies regulated pressure to a single chamber of the pneumatic cylinder (Fig. 4). This enables the pressure difference across the cylinder to be specified by software changes alone and also allows the individual chamber pressures to be regulated by the valves themselves, avoiding the need for additional pressure control that has been implemented, for example, in Ref. [22]. To achieve accurate control, it is desirable to control both valves from a single control signal. This has been achieved through the use of an equilibrium pressure for which one valve has pressure increased and the other valve has pressure decreased [14]. Thus, through manipulation of a single control voltage, the output force and, hence, link position can be altered. Analysis of pneumatic systems has been performed for many years; however, only recently with proportional valves and low friction cylinders can pneumatics be considered for precision applications. One of the first people to analyze moving pneumatic systems was Shearer [23], who developed a detailed model of a double-ended cylinder by considering both isothermal and adiabatic heat transfer processes. Also, Liu and Bobrow [22] controlled a simple 1-d.o.f. pneumatic robot, experimentally determining linearized spool valve coefficients and developing a control algorithm around the model. McDonnell [24] developed a model of a pneumatic cylinder and spool valve using established techniques, forming experimental quadratic models of mass flow. Research has been performed into the behavior of asymmetric actuators. Wong and Moore [25] analyzed the behavior of double-ended asymmetric cylinders when driven from a single end. They found significant differences in maximum response time, velocity, acceleration and force for extension and retraction. The modern pneumatic system implemented here uses valves with internal pressure regulation and low-friction

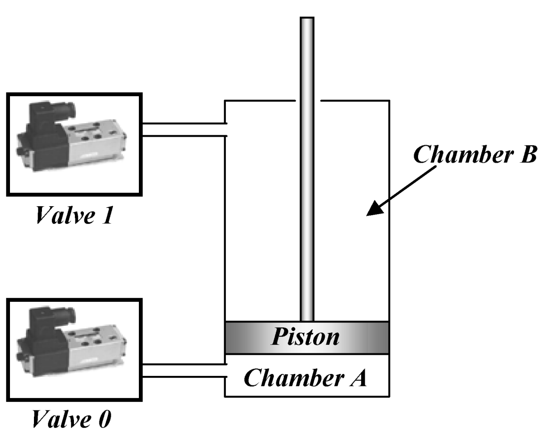

Figure 4. The valve and cylinder arrangement.

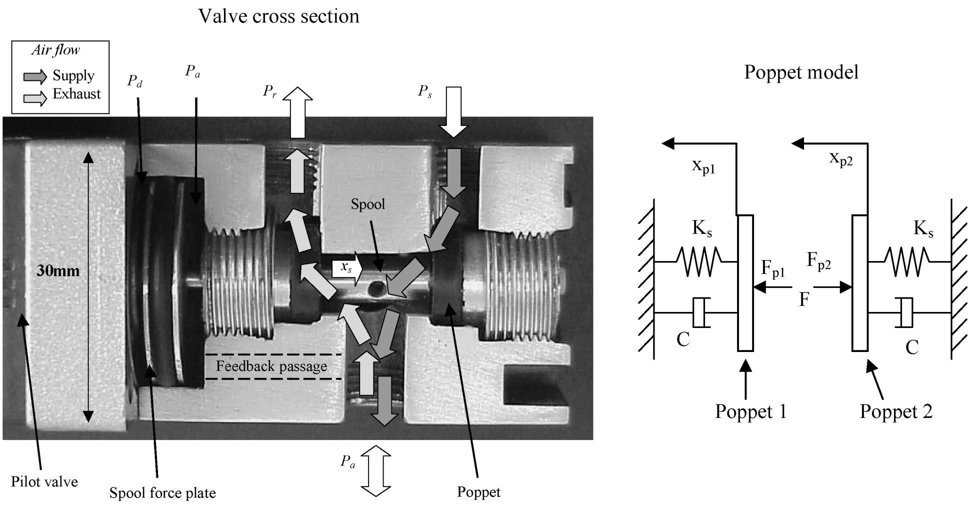

Figure 5. The valve and cylinder arrangement.

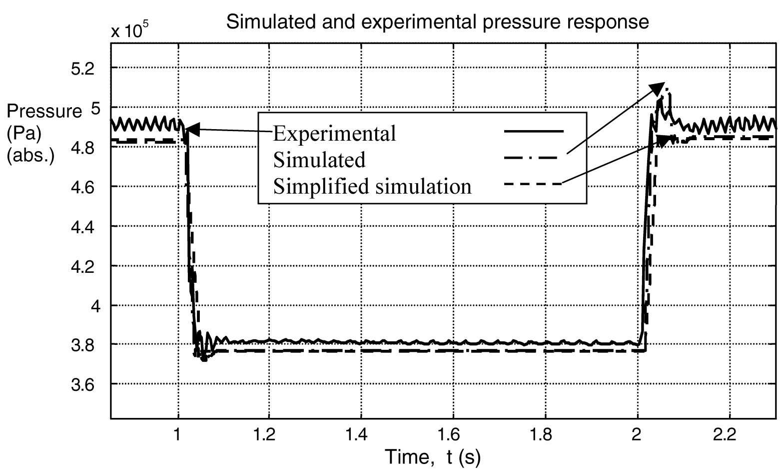

Figure 6. Simulated and experimental pressure response.

cylinders. Therefore, analysis of the pneumatic system was required to understand its performance. Previous work has assessed the performance of the low-friction pneumatic cylinder [18]. Here, analysis of the valves will be discussed.

The cylinder displacement was fixed at its mid-point while a single valve was used to supply pressure to the bottom chamber. The valves are designed so that pressure output is proportional to voltage input. Examining the structure of the valve (Fig. 5), a controlled pilot stage supplies pressure proportional to voltage into a small volume. The pressure difference between pilot pressure (P_d) and actual pressure (P_a) moves the spool, which in turn operates the poppet valves.

The step response obtained from the valve was compared with a simulated response [26] (Fig. 6). The response time of the simulation closely matches that of

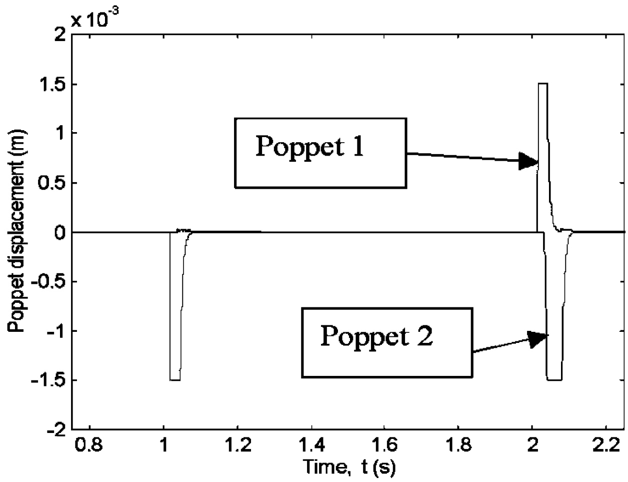

Figure 7. Simulated poppet displacement at transient point of the response.

the experimental. The general shape of the overshoot agrees with the experimental results. Note the oscillations of the experimental result are due to measurement noise. It is apparent from inspection that the pressure overshoot for supply is greater than exhaust. This is due to the difference in supply pressure and chamber pressure (P_s and P_a). For example, with $P_a = 4.5$ bar (abs.) and saturation of orifice area due to pipes, the maximum mass flow rate for supplying air is 1.5-times larger than the mass flow rate for exhausting air even though air entering the chamber is slightly unchoked. As both poppets have the same delay in closing, a larger pressure overshoot is created when supplying pressure.

Examining the poppet displacements (Fig. 7) at approximately 2 s, for a pressure increase, illustrates the valves operation:

(i) Poppet 1 opens due to desired pressure being greater than actual pressure.

(ii) Due to overshoot in pressure, poppet 2 opens.

(iii) Poppet 1 closes (lag due to damping).

(iv) Then poppet 2 closes (again with lag).

Note that the delay in poppet closing allows both poppets to be open simultaneously.

Due to the overall bandwidth of the pneumatic robot, these transient pressure spikes do not affect the overall performance.

2.3. Force sensor

It is important to know the interaction forces between the robot and human at all times for two reasons: the interaction force needs to be monitored to ensure excessive forces are not applied to the human and measurement of the applied force is required to implement the impedance control strategy. A custom 3-d.o.f.

force sensor has been developed for this purpose; however, the force sensor misread torque as applied force, resulting in poor performance [21]. A commercial force sensor measuring contact forces in 6-d.o.f. has been implemented on the robot. The robot is only capable of applying forces in 3-d.o.f.; however, the interaction with a human arm results in greater d.o.f. being active at the point of contact. The sensor allows the applied torque to be monitored for comfort and safety.

3. IMPEDANCE CONTROL

Impedance control has been developed over the last decade to enable robots to smoothly move between contact and non-contact phases of motion. Examining how humans interact with their environment was an integral part of this development. Impedance control fixes the relationship between the manipulator end-point and external disturbances. In position based impedance control, the impedance controller alters the position for any force applied to the robot end-point.

Impedance control utilizes a mass, spring and damper relationship between force and position (Fig. 8). The transfer function connecting force and position used in position based impedance control (admittance control), can be specified in the s-domain as:

$$\frac{x_{\mathrm{i}}}{F_x} = \frac{1}{Ms^2 + Cs + K}, \tag{1}$$

where x_{i} is the change in position due to external force (F_x), M is the inertial component, C is the damping component and K is the stiffness component.

Rearranging (1) so that position becomes the input, known as force-based impedance control, gives:

$$\frac{F_x}{x_{\mathrm{i}}} = Ms^2 + Cs + K. \tag{2}$$

Equations (1) and (2) are known as the duality of impedance control. These two subtly different approaches require different controller structures. A more detailed

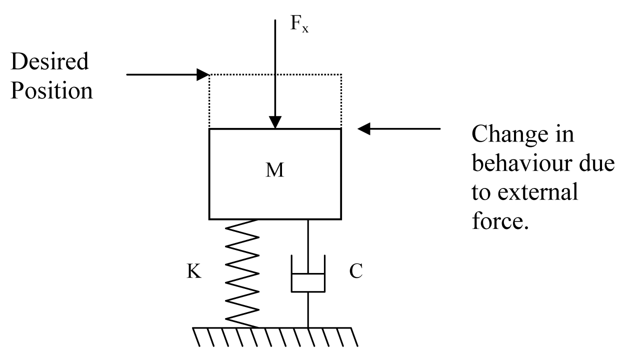

Figure 8. Impedance control free body diagram.

Table 2.
Comparison of admittance control and impedance control

	Admittance control	Impedance control
Advantages	most appropriate for environments consisting of stiffness and damping elements	most appropriate for environments consisting of inertial element
	only requires addition of a force sensor on conventional robotic devices based around measurement of link position	easy to implement on direct-drive electric motor systems due to the ease at which torque can be controlled during motion
Disadvantages	requires a high gain position controller robust to external force disturbances	difficult to implement on actuator systems where force output is effected by robot movement
		requires robot inertial model, which can be difficult to obtain

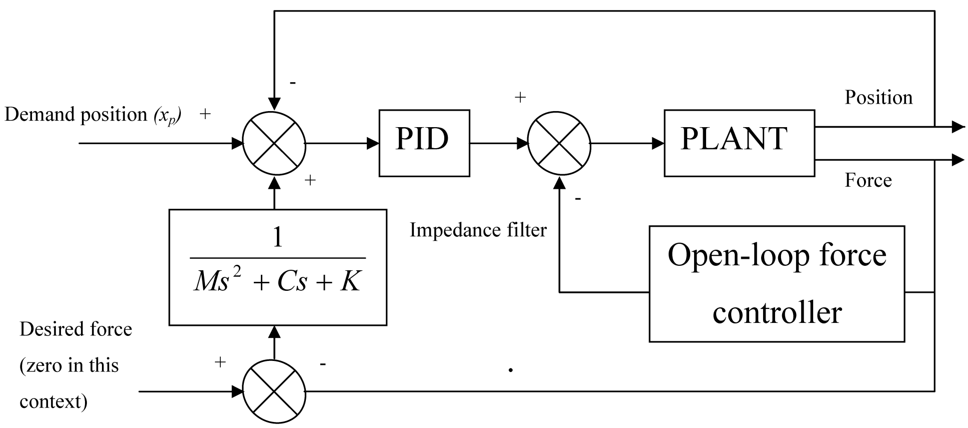

Figure 9. Impedance controller block diagram.

discussion of these differences can be found in Ref. [27], but a summary of the advantages and disadvantages of each type of impedance controller is given in Table 2. As highlighted by Ref. [17], position-based impedance control (admittance control) is more appropriate for pneumatic systems.

The position controller described earlier is not robust to external forces. However, it was demonstrated in the force control section that open-loop force control is effective for fixed position force control. Combining the position controller and open-loop force controller greatly increases the controller's ability to reject force disturbances. The overall impedance control strategy is shown in Fig. 9 (for a single link).

3.1. Impedance control implementation

A flow chart of the multiple-d.o.f. controller is shown in Fig. 10. The desired end-point trajectory is specified before implementing the controller, in the form

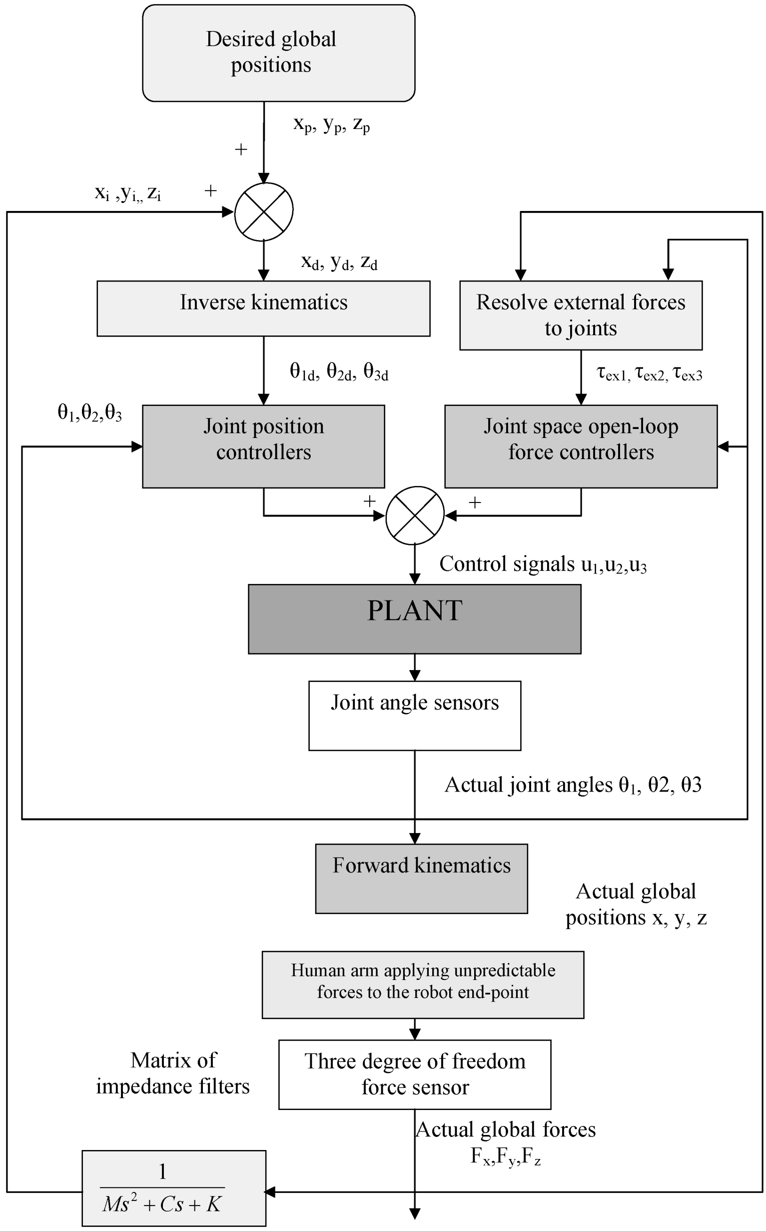

Figure 10. Implementing impedance control in multiple d.o.f.

of global position coordinates (x_p, y_p, z_p). These coordinates, when added to the desired change in position due to external forces (as a result of the impedance filter) (x_i, y_i, z_i), form the desired robot position at any instant. The desired global positions are converted into joint space demands ($\theta_{1d}, \theta_{2d}, \theta_{3d}$), using the robot inverse kinematics. Three independent controllers implement the desired joint space positions.

External forces are resolved through the robot to obtain their influence on each joint ($\tau_{ex1,} \tau_{ex2,} \tau_{ex3}$). An equal, but opposite force is generated by the joint space open-loop force controllers, to reduce the effects of these external forces on link position.

The forward kinematics of the joint positions reveal the robot end position in task space coordinates (x, y, z). External forces are measured at the robot end-point using the 3-d.o.f. force sensor. Three separate impedance filters convert the global external forces F_x, F_y and F_z into changes of the x, y and z desired task space coordinates, respectively. Note that it is possible to implement different impedance filters for different d.o.f. enabling one d.o.f. to be stiff while another is compliant.

The impedance controller with damping and stiffness has been experimentally implemented on all 3-d.o.f. of the pneumatic robot. To assess the controller performance, five alternative stiffness and damping parameters were assessed. Due to the inertia of the robot links and delays in the robot response it is not possible to implement zero damping and stiffness (this would result in zero force for any movement of the robot end-point).

Beginning with low stiffness and damping ($K = 50$, $C = 50$) (Fig. 11), the required trajectory for both position and velocity is accurately tracked, with only

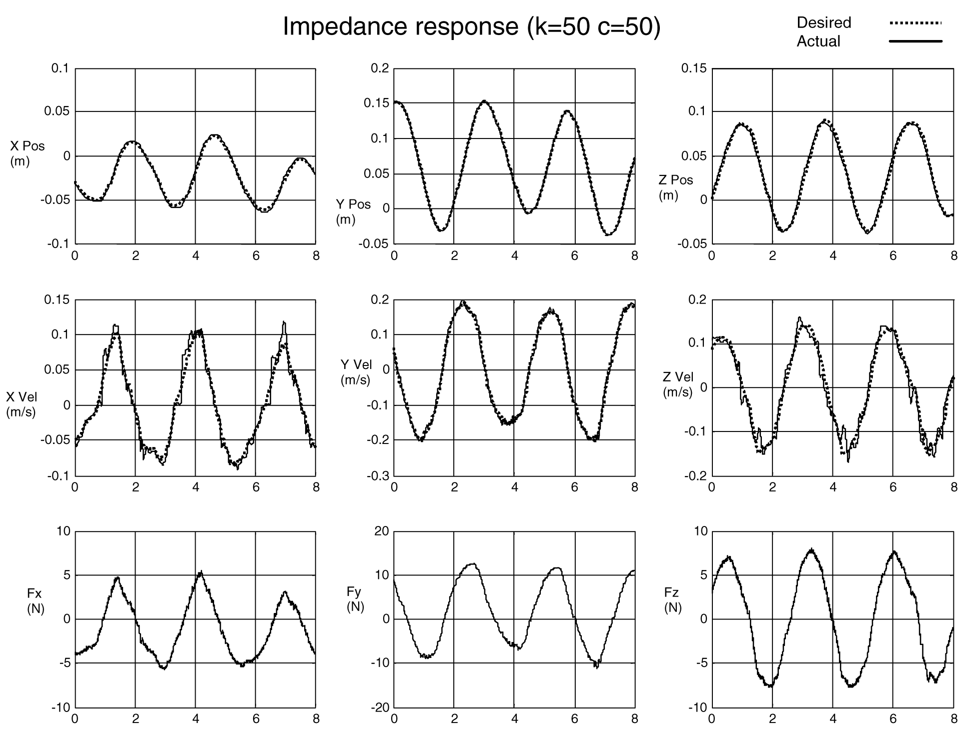

Figure 11. Impedance response ($K = 50$, $C = 50$).

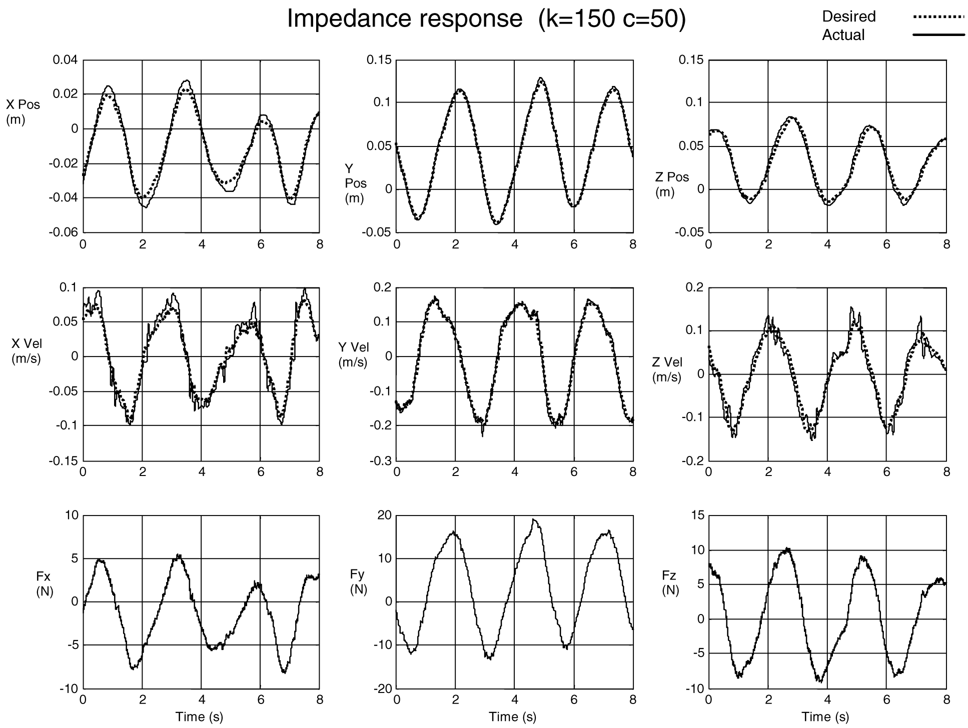

Figure 12. Impedance response ($K = 150$, $C = 50$).

minimal noise evident on the velocity response. The damping term causes the position demand to lag the force input, causing a delay between a peak in force and the resultant peak in displacement.

Using a medium-high stiffness with low damping ($K = 150$, $C = 50$) (Fig. 12) sees a slight decrease in tracking performance, although less significantly in the y-axis since this is predominantly affected by the motion of just one joint. Increasing damping and retaining medium stiffness ($K = 100$, $C = 200$) (Fig. 13) results in larger tracking errors, particularly in velocity. Using a high stiffness and low damping ($K = 500$, $C = 50$) (Fig. 14) puts a high demand on the system and consequently results in the poorest performance. The degradation in the velocity response is most pronounced, especially in the x- and z-axes. With stiffness as the dominant factor in the impedance controller the position demand is in phase with the force input, with peaks in applied force relating to peaks in displacement. It is important to realize the performance of the controller is dependent upon the desired impedance parameters. Figure 15 shows the %RMS error for different values of stiffness.

It is evident that increasing stiffness in the controller will result in greater tracking errors in both position and velocity. The effect played by damping is dependent upon the frequency of the input force; however, it is reasonable to assume that the same trend exists when increasing the damping factor for a constant frequency force

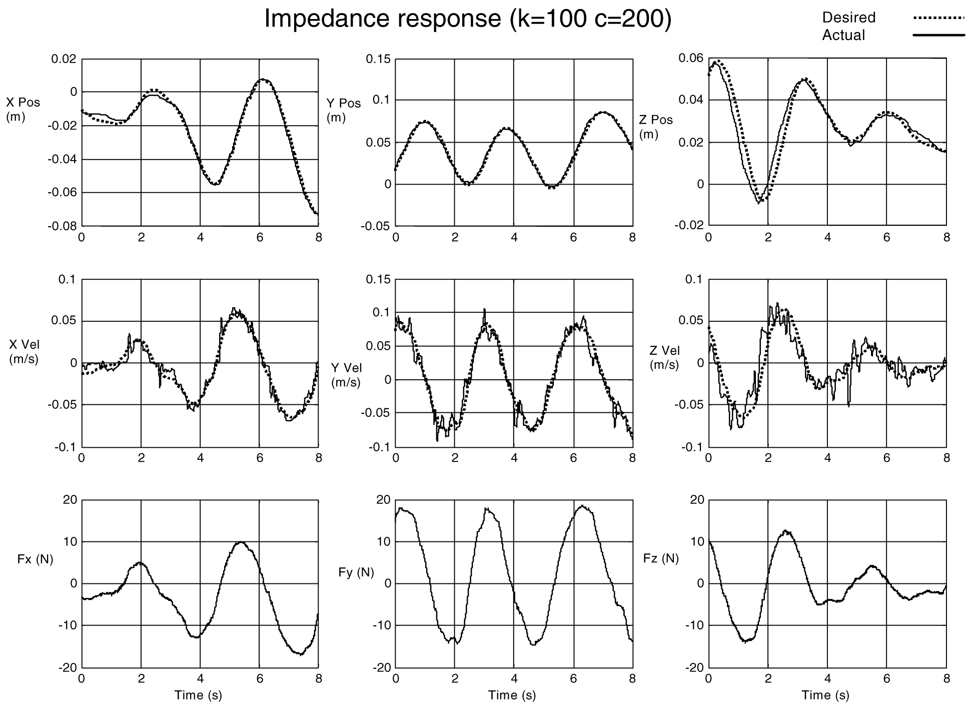

Figure 13. Impedance response ($K = 100$, $C = 200$).

input. When the tracking errors become too large the system will cease to behave reliably as a spring–damper. Imposing an upper limit on the admittance controller parameters will help limit these errors and ensure reliable operation.

3.2. Description of robot physiotherapy

The impedance control strategy is crucial to the implementation of robotic physiotherapy. The exercise strategy is to coordinate arm motion towards therapeutically defined points, as indicated on a computer screen. Any trajectory error is assisted by forces depending upon the specified impedance parameters. Through the implementation of relatively high stiffness (e.g., $k = 400$) users with very inhibited motion will be able to exercise. More able users will exercise with reduced stiffness parameters resulting in smaller forces being applied to assist their motion by correcting trajectory errors. Damping parameters can be adjusted to resist any involuntary shaking and provide a smooth motion. During an exercise regime the impedance values would be reduced (over a period of months) as arm movement improves.

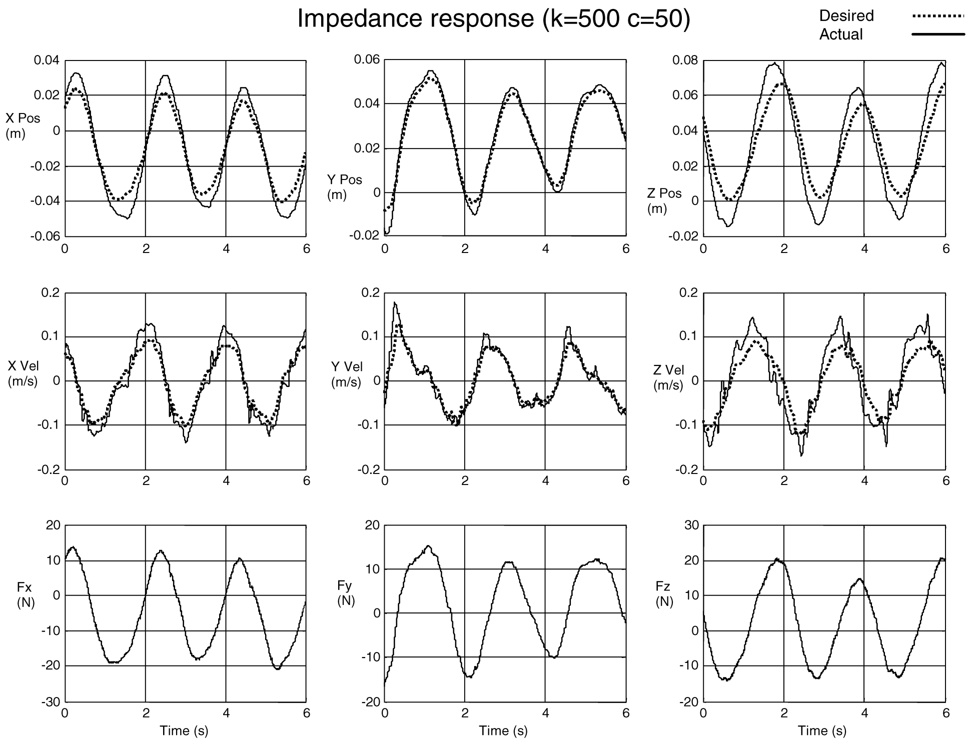

Figure 14. Impedance response ($K = 500$, $C = 50$).

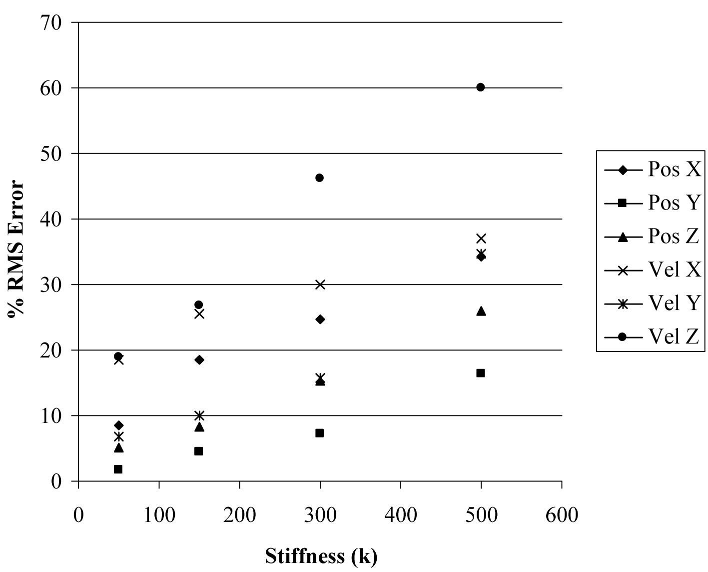

Figure 15. %RMS error for different values of stiffness.

4. DISCUSSION AND CONCLUSIONS

A 3-d.o.f. robot has been designed and constructed that is capable of administering robotic physiotherapy. To measure interaction forces a commercial 6-d.o.f. force sensor acts as the interface between the robot and human. The results of tests varying stiffness and damping parameters show the performance to vary, degrading with increasing parameters.

The final application of the device is to implement robotic physiotherapy. An important part of this is to apply gravity compensation to a patients arm; the weight of a patients arm is a significant barrier to exercise in those with severe disability. Figure 16 shows a test performed on an able-bodied subject making use of the controllers ability to implement different impedance parameters in different axis. In this case the axis that is required to support the weight of gravity has 4 times the amount of stiffness. The graphs show that the controller was able to apply a force between 10 and 20 N in the direction of gravity whilst applying more subtle assistance in the other d.o.f.

The final robot has the potential to administer physiotherapy; however, the quality of the force measurement needs to be improved before any patient trials can be performed. Further work will improve the controller performance and test the robot on a few sample patients.

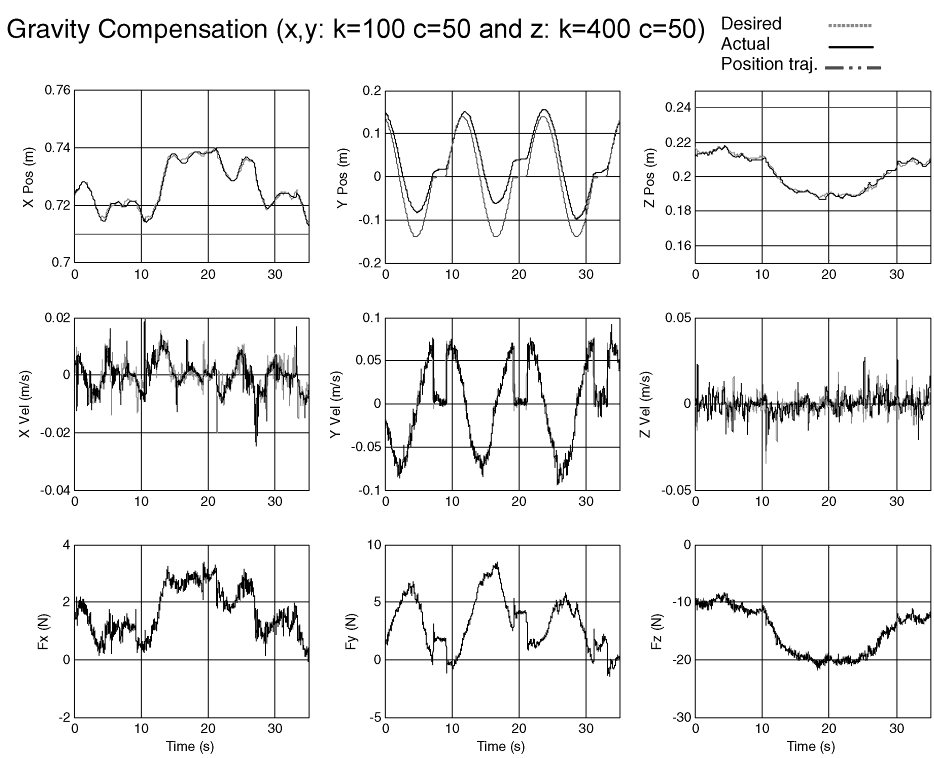

Figure 16. Arm gravity compensation.

REFERENCES

1. J. M. Bamford, P. Sandercock, M. Dennis, C. Warlow, L. Jones, K. McPherson, M. Vessey, G. Fowler, A. Molyneux, T. Hughes, J. Burn and D. Wade, A prospective study of acute cerebrovascular disease in the community: the Oxfordshire Community Stroke Project 1981–1986: methodology, demography,and incident cases of first ever stroke, *J. Neurol. Neurosurg. Psychiatry* **51**, 1373–1380 (1988).
2. G. Kwakkel, R. C. Wagenaar, J. W. R. Twisk, G. J. Lankhorst and J. C. Koetsier, Intensity of leg and arm training after primary middle cerebral artery stroke: a randomised controlled trial, *Lancet* **354**, 191–196 (1999).
3. A. Sunderland, D. J. Tinson, E. L. Bradley, D. Fletcher, R. Langton Hewer and D. T. Wade, Enhanced physical therapy improves recovery of arm function after stroke. A randomised controlled trial, *J. Neurol. Neurosurg. Psychiatry* **55**, 530–535 (1992).
4. P. Pound, C. Sabin and S. Ebrahim, Observing the process of care: a stroke unit, elderly care unit and general medical ward compared, *Age and Ageing* **28**, 433–440 (1999).
5. J. A. Cozens, Robotic assistance of an active upper limb exercise in neurologically impaired patients, *IEEE Trans. Rehabil. Eng.* **7**, 254–256 (1999).
6. H. Krebs, N. Hogan, M. Aisen and B. Volpe, Robot-aided neurorehabilitation, *IEEE Trans. Rehabil. Eng.* **6**, 75–87 (1998).
7. M. A. Buckley, A. Yardley, R. G. S. Platts and S. S. Marchese, MULOS system prototype. *http://www.ncl.ac.uk/crest/Prototype.htm#specification*.
8. K. Nagai, I. Nakanishi and H. Hanafusa, Development of an 8 DOF Robotic orthosis for assisting human upper limb motion, in: *Proc. IEEE Int. Conf. on Robotics and Automation*, Leuven, pp. 3486–3491 (1998).
9. M. H. Raibert and J. J. Craig, Hybrid position/force control of manipulators, *ASME J. Dyn. Syst., Meas. Control* **103**, 126–133 (1981).
10. S. Chiavervini and L. Sciavicco, The parallel approach to force/position control of robotic manipulators. *IEEE Trans. Robotics Automat.* **9**, 361–373 (1993).
11. N. Hogan, Impedance control: an approach to manipulation part I, II, III, *J. Dyn. Syst., Meas. Control* **107**, 1–24 (1985).
12. E. Richer and Y. Hurmuzlu, High performance pneumatic force actuator system: part I & II, *Trans. ASME* **122**, 416–425 (2000).
13. J. Wang and Y. Y. Lin-Chen, Modelling study, validation and robust tracking control of pneumatic cylinder actuator systems, presented at: *UKACC Int. Conf. of Control*, Cambridge (2000).
14. R. Richardson, A. R. Plummer and M. D. Brown, Self-tuning control of a low friction pneumatic actuator under the influence of gravity, *IEEE Trans. Control Syst. Technol.* **9**, 330–334 (2001).
15. B. W. McDonell and J. E. Bobrow, Modelling, identification and control of a pneumatically actuated robot, in: *Proc. IEEE Int. Conf. on Robotics and Automation*, Alburquerque, NM, pp. 124–129 (1997).
16. P. Gorce and M. Guihard, Joint impedance pneumatic control for multilink systems, *ASME J. Dyn. Syst., Meas. Control* **121**, 293–297 (1999).
17. B. Heinrichs, N. Sepehri and A. B. Thorton-Trump, Position-based impedance control of an industrial hydraulic manipulator, *IEEE Control Syst. Mag.* **17**, 46–52 (1997).
18. R. Richardson, M. D. Brown and A. R. Plummer, Pneumatic impedance control for physiotherapy, in *Proc. EUREL Int. Conf. on Robotics*, Salford, Vol. 2 (2000).
19. R. Richardson, M. E. Austin and A. R. Plummer, Development of a physiotherapy robot, in *Proc. Int. Biomechatronics Workshop*, Enshede, pp. 116-120 (1999).
20. E. J. McCormick, *Human Factors Engineering*. 3rd. edn. McGraw-Hill, New York (1970).
21. R. Richardson, M. D. Brown, B. Bhakta and M. Levesley, Design and control of a three degree of freedom pneumatic physiotherapy robot, *Robotica* **21**, 589–604 (2003).

22. S. Liu and J. E. Bobrow, An analysis of a pnuematic servo system and it's application to a computer-controlled robot, *Trans. ASME J. Dyn. Syst. Meas. Control* **110**, 228–235 (1988).
23. J. L. Shearer, Study of pneumatic processes in the continuous control of motion with compressed air I, II, *Trans. ASME* **Feb.**, 233–249 (1956).
24. B. McDonnell, Modelling, identification, and control of a pneumatically actuated robotic manipulator, *PhD Thesis*. University of California–Irvine (1996).
25. P. J. Wong and P. R. Moore, Acceleration characteristics of a servo controlled pneumatic cylinder, *ASME Fluid Power Syst. Technol.* **3**, 119–130 (1996).
26. R. Richardson, M. D. Brown, B. Bhakta and M. Levesley, Modelling and simulation of a precision pneumatic actuation system, presented at *Multi-body Dynamics: Monitoring & Simulation Techniques*, Loughborough (2004).
27. R. C. Richardson, Control and actuation for robotic physiotherapy, *PhD Thesis*. University of Leeds (2001).

ABOUT THE AUTHORS

Robert C. Richardson received the BE degree in Mechatronics from the University of Leeds, UK, in 1997. In July 2001, he obtained a PhD from the University of Leeds, UK, for a thesis titled 'Actuation and control for a physiotherapy robot'. His thesis involved the application of neurologically based controllers on a novel robot design to encourage recovery of the upper-limb after stroke. In April 2003, he took up the post of Lecturer in Robotics, Department of Computer Science, University of Manchester, UK, as part of the Artificial Intelligence Group. He is currently responsible for the undergraduate and MSc courses in robotics. His current research interests include rehabilitation robotics, robot and human interaction, urban search and rescue robots, modern actuator systems, and advanced control systems.

Bipin Bhakta is Head of the Academic Department of Rehabilitation Medicine within the Faculty of Medicine and Health, University of Leeds, UK. Over the last 10 years his research activity has spanned development of restorative rehabilitation technologies, clinical trials, qualitative research, health outcome and educational assessment, and vocational rehabilitation research.

Martin C. Levesley received the BE degree in Mechanical Engineering from Brunel University, Brunel, UK, in 1988, and the PhD degree (working on efficient computation and experimental assessment of squeeze film damper response), from the University of Southampton, Southampton, UK, in 1992. He was a Senior Research Fellow at the University of Southampton, where his research continued to focus on the nonlinear modeling and control of motion in aero-engine rotor structures. In 1997, he joined the University of Leeds, UK, as a Lecturer, teaching dynamics and control, where his research interests broadened to include the analysis and control of motion in smart structures, smart self-sensing actuators, automotive systems, and robotic devices.

Andrew Jackson completed a Mechatronics BE degree at the University of Leeds in 1999. This was followed by a PhD at the same institution in 2004 working in the field of vehicle dynamics and control. His work focused on individual wheel control of a 6×6 hybrid electric off-road vehicle incorporating traction control, anti-lock braking and direct yaw-moment control. He is currently a Research Associate at the School of Mechanical Engineering where his main interest lies in rehabilitation robotics.

Pete Culmer completed a Mechatronics ME degree at the University of Leeds in 2002. He is now studying at the University of Leeds where he is currently working towards a PhD in the Department of Mechanical Engineering. The PhD concerns the development of a robotic device for upper-limb stroke rehabilitation.